# Elastic constants of neon single crystals determined by Brillouin scattering*

R. A. McLaren,† H. Kiefte,‡ D. Landheer,§ and B. P. Stoicheff
*Department of Physics, University of Toronto, Toronto, Ontario, M5S 1A7, Canada*
(Received 9 September 1974)

High-resolution Brillouin spectroscopy has been used to determine the adiabatic elastic constants of solid neon at 24.3 K. Single crystals were grown for this investigation, and laser-excited spectra were recorded for various crystal orientations. The observed spectra included the longitudinal Brillouin doublet and, usually, the low-frequency transverse doublet. Their frequency shifts for eight different single crystals were used to obtain the following values for the adiabatic elastic constants (in kbar): $C_{11} = 11.70 \pm 0.21$, $C_{12} = 7.31 \pm 0.17$, and $C_{44} = 6.02 \pm 0.15$. From these values, it is found that the elastic anisotropy parameter $A = 2.74 \pm 0.10$, and the adiabatic bulk modulus $B_s = 8.77 \pm 0.17$ kbar. The best agreement between these experimental values of the elastic constants and theoretical values is obtained for quasiharmonic calculations using a Mie-Lennard-Jones (6-12) all-neighbor potential.

## I. INTRODUCTION

Brillouin spectroscopy has recently been used by Gornall and Stoicheff[1] to determine the adiabatic elastic constants of solid xenon at the triple point. Following this initial success, our laboratory began a long-range program for studying the Brillouin spectra of all of the rare-gas solids, and investigations were started on argon,[2,3] neon,[2] and krypton[4] crystals. This paper describes in detail the experiments with neon single crystals, and the determination of the adiabatic elastic constants of neon at the triple point. The present work is the first known study of the Brillouin spectrum of solid neon.

Solid neon is one of the most interesting of the rare-gas solids since its properties are intermediate between those of helium, which is a true quantum solid, and those of argon, krypton, and xenon, which are basically classical solids. In solid helium, the large zero-point atomic displacements (~30% of the nearest-neighbor distance) make the inclusion of short-range correlations essential to an adequate description of its lattice dynamics.[5] The atomic displacements in neon (~9% of the nearest-neighbor distance at 0 K) are sufficiently smaller than those in helium so that short-range correlations become negligible[6] but are still large enough for pronounced anharmonicity even at 0 K. For this reason, neon has always been of special theoretical significance.[7] Furthermore, recent spectroscopic[8] and molecular-beam[9,10] experiments have provided precise information on the pair interaction between neon atoms. This has prompted renewed theoretical interest[10-12] in solid neon with the aim of answering the following two basic questions: (a) Can these accurate pair potentials be used to calculate solid-state properties? (b) What is the role of many-body forces[13-16] (nonpairwise additive forces) in solid neon and how may these forces be described? Experimental values of the elastic constants will be valuable in answering these questions, and consequently, a measurement of these constants is particularly appropriate at the present time.

The present experiment with neon was similar to that of Gornall and Stoicheff[1] with xenon, and of Gewurtz and Stoicheff[3] with argon. However, the particular properties of solid neon did necessitate several basic changes in the apparatus. First of all, neon solidifies under its own vapor pressure at a temperature of 24.55 K (the triple point), and therefore liquid-helium cryogenics was required. Furthermore, the small polarizability of the neon atom results in a very low-Brillouin-scattering cross section for the solid, ~100 times lower than that for solid xenon. Consequently, it was necessary to use a high-powered argon laser to excite the scattering and to employ a sophisticated Fabry-Perot spectrometer coupled to a digital memory to record the spectra. Finally, the low x-ray scattering efficiency of solid neon necessitated careful design of the sample cell to minimize the x-ray background.

In the present investigation, eight neon single crystals were grown and studied at the triple point. Experience has shown that it is easiest to grow single crystals at the triple point, and moreover, this is the most interesting region for study since it is here that the effect of anharmonicity is the greatest. The quality of the crystals and their orientations were determined by transmission Laue x-ray diffraction, as in the earlier experiments with xenon and argon. Brillouin spectra at a scattering angle of 90° were recorded for several orientations of each crystal, with the temperature maintained at 24.3 K. The observed spectra exhibited the longitudinal and, usually, one transverse component. Their frequency shifts were then used to determine the values of the adiabatic

elastic constants to an accuracy better than ±2.5%.

Since the relevant theory and the experimental method have been given in considerable detail in the earlier papers,[1,3] only the new developments in experimental technique and data analysis will be described here. These include the helium Dewar and sample cell, the spectrometer and detection system, and an iterative procedure for obtaining values of the elastic constants and their errors from the experimental data.

## II. EXPERIMENTAL APPARATUS AND TECHNIQUE

### A. Liquid-helium cryostat and sample cell

A schematic diagram of the complete experiment is shown in Fig. 1. Single crystals of neon were grown in a cylindrical Plexiglas cell which was suspended vertically in the tail section of a helium cryostat (Andonian model 024/7M). In this cryostat, liquid helium is admitted from the reservoir to a vaporizer in the sample zone and cooling is provided by the flow of gas from the vaporizer. The details of the specially designed tail section of the cryostat are shown in Fig. 2. The vaporizer was attached to a tubular copper cold finger which served as a reservoir of cold gas. The sample cell was suspended from a 1-m length of thin-wall stainless-steel tubing which also served as the filling line. A pointer attached to the tube, and a protractor dial mounted on a rotary seal indicated the angular position of the cell.

The sample cell was surrounded by two gold-plated radiation shields: The inner one consisted of the cold finger and a $U$-shaped shroud attached to it, and the outer shield was suspended from the liquid-nitrogen reservoir. An optical-quality fused quartz window at the bottom of the cryostat served as the entrance window for the laser beam. The x-rays entered from the side through a Plexiglas window. A second Plexiglas window transmitted the scattered light and x rays (up to scattering angles of 30°). Rubber O rings were used to seal the Plexiglas windows to the outer envelope of the cryostat.

Figure 3 is a detailed drawing of the sample cell. The cylindrical cell body was made of Plexiglas and had an inner diameter of 2.5 mm, a wall thickness of 0.5 mm, and an over-all length of 20 mm. The main reasons for using Plexiglas were its low x-ray absorption coefficient and its low thermal conductivity. This latter property was important because it forced the heat of fusion to be extracted through the growing crystal rather than through the cell walls, thereby preventing stray nucleation on the walls. Careful machining and annealing of the cell were essential to prevent cracking at low temperature. The laser beam entered the cell through a cylindrical fused-quartz window 2 mm in diameter and 6 mm in length whose end faces were highly polished to minimize parasitic scattering. This window was cemented with epoxy inside the copper end piece at the bottom of the

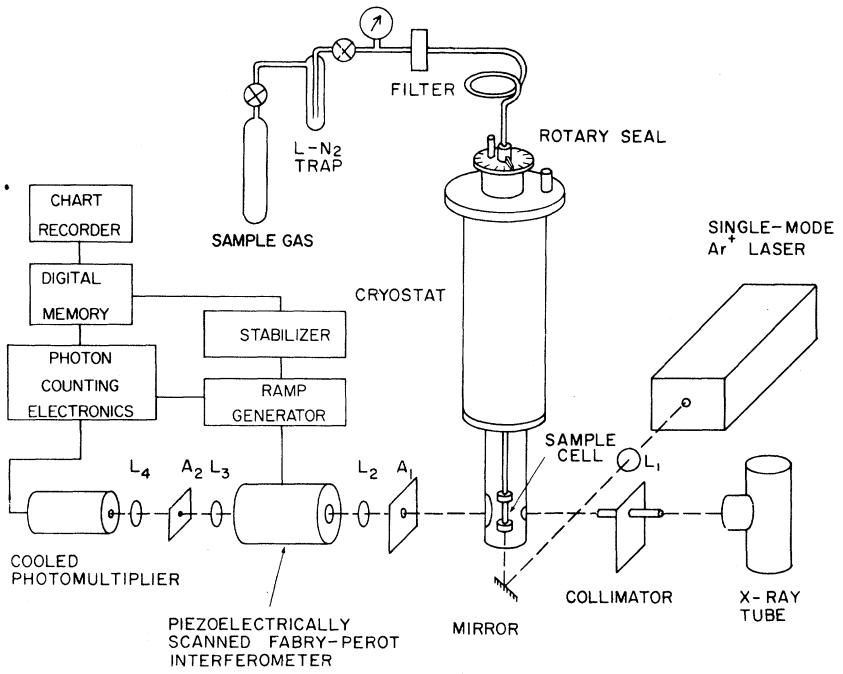


FIG. 1. Experimental arrangement for Brillouin scattering and x-ray diffraction of neon single crystals.

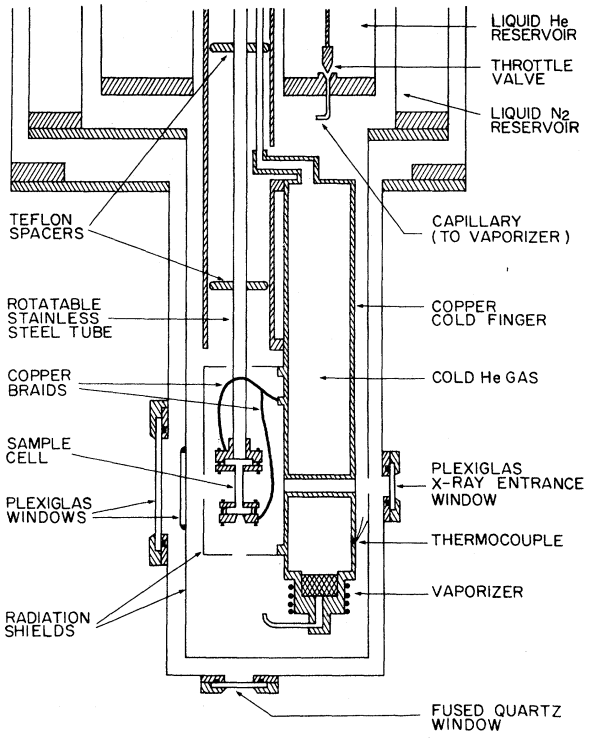


FIG. 2. Cryostat tail section.

cell. The seal between the end piece and cell body was made with an indium O ring. At its top the sample cell was attached to the stainless-steel tube by means of a copper fitting and a second indium O ring seal. Considerable care was taken during the assembly of the sample cell to ensure that the window surfaces were scrupulously clean, since even a small amount of contamination could produce sufficient parasitic scattering to obscure the weak transverse components in the Brillouin spectrum.

The cell was cooled by conduction through four copper braids. Two of these were soldered to the fitting at the top; the other two to the end piece at the bottom (Fig. 3). At the top of the cell, a 50-Ω heater was wound around the fitting and also around the first 5 cm of the supporting tube. At the bottom, 25-Ω heaters were wound on opposite sides of the end piece and connected in series, and the temperature was measured by a copper-constantan thermocouple. A voltmeter null detector (Fluke model 845AB) measured the difference between the thermocouple emf and the voltage obtained from an adjustable set-point circuit. The null-detector output was used to regulate the current supplied to the cell heaters. The current was divided between the top and bottom heaters by means of a potentiometer; this permitted the temperature at the bottom of the cell to be maintained within 50 mK of the set point while the temperature at the top was held constant to an accuracy of 100 mK. The temperature difference across the cell could be adjusted by changing the potentiometer setting, and was monitored with a differential thermocouple.

### B. Crystal growth and orientation

The neon gas was supplied by the Matheson Co. in the natural isotopic abundance (91% $^{20}$Ne, 9% $^{22}$Ne) and with a nominal purity of 99.995%. Their analysis stated that the only impurity above 1 ppm was 3 ppm of helium. The gas was admitted to the cell through a liquid-nitrogen cold trap (see Fig. 1), and a Millipore filter (0.22 $\mu$m) to prevent dust from entering the cell. Prior to each experiment, the sample cell and gas-handling system were evacuated to a pressure of ~$10^{-5}$ Torr.

Single crystals were grown by the following technique.[17] With the cell temperature stabilized at 26 K, neon gas was allowed to enter until the cell was full of liquid. By adjusting the heater potentiometer a temperature differential of ~0.5 K was established between the top and bottom of the cell (top hotter). The temperature was then lowered while maintaining this differential until a "seed" crystal ~1 mm high formed on the window. Solidification occurred at the triple point (24.55 K), and this was used to calibrate the thermocouple. After the "seed" had been annealed for ~1 h, a Laue photograph was taken to ascertain whether or not it was a single crystal. If the "seed" was poly-

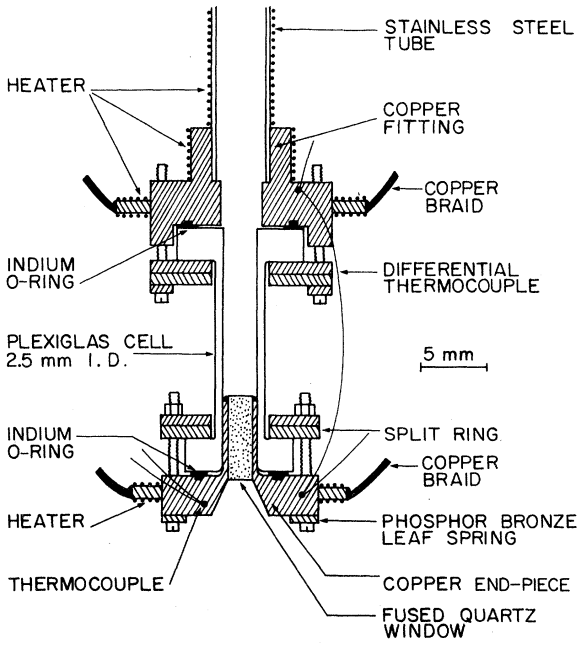


FIG. 3. Sample cell for growing neon single crystals.

crystalline (as was the case for ~90% of the attempts), it was melted and another one grown. When a single-crystal "seed" was obtained, it was annealed for several hours more. The temperature was then slowly decreased until the crystal had grown to the desired length of ~7 mm. Growth rates ranged from 0.5 mm/h to 1 mm/h. After crystal growth had been completed, the cell temperature was left unchanged for the duration of the experiment. Parasitic scattering from the upper surface of the crystal was minimized by leaving a few millimeters of liquid above the solid; the liquid was in equilibrium with the vapor at a pressure of ~400 Torr. The temperature in the scattering volume, midway up the cell, could not be measured directly but was estimated to be 24.3 ± 0.2 K. This was based on the temperature differential of 0.4 K, which was maintained between the ends of the crystal, and on the fact that the solid-liquid interface had to be at the triple point.

The crystal orientation was determined as described in the earlier work on argon.[3] The x-ray beam had a diameter of 2.5 mm at the sample cell, sufficient to probe the entire breadth of the crystal. Transmission Laue photographs were taken for each orientation of the eight crystals, and the positions of the diffraction spots were used to determine the Euler angles $(\theta, \phi, \chi)$ which specified the orientation of the crystal axes with respect to the laboratory-fixed axes. Once this was known, it was a simple matter to calculate the direction of the scattering vector $\vec{q}$ and the polarization of the incident laser radiation $\vec{E}_0$ in the crystal reference frame.

The possibility of there being a preferred crystal orientation with respect to the direction of growth (that is, with respect to the cell axis) was investigated. Figure 4 shows the growth direction plotted on a stereographic projection of $\frac{1}{48}$ of the reference sphere. It can be seen that the crystals tended to grow with a ⟨110⟩ direction aligned with the cell axis, although not with a high degree of reproducibility.

### C. Light scattering and spectrometer

The exciting radiation at 4879.9 Å was produced by a single-mode $Ar^+$ laser (Coherent Radiation 52B). Careful attention to the acoustic environment of the laser led to considerably improved frequency stability. Thus, the emitted radiation had a short-term frequency jitter of only ±15 MHz, and only a few mode hops per day. Although thermal drift could not be eliminated, compensation was provided by a stabilization technique especially designed for this purpose and described by McLaren and Stegeman.[18]

The laser output was attenuated by neutral density filters to 50 mW and directed into the cryostat by a first-surface mirror (Fig. 1). Lens $L_1$ ($f = 200$ mm) focussed the beam to a diameter of ~0.2 mm at the center of the cell. A small adjustment of the beam position in the cell was usually necessary in order to minimize parasitic scattering from microscopic imperfections in the crystal and from the liquid meniscus. Consequently, the scattering volume often did not lie precisely on the axis of the cell. This, in conjunction with the curvature of the cell walls, produced a slight refraction of the scattered light. However, calculations based on the cell geometry and on the refractive indices of solid neon ($n = 1.107$, see Appendix) and of Plexiglas ($n = 1.50$) showed that this effect was negligible ($< 0.5°$ deviation). After the beam position had been optimized, the image of the scattering volume was set exactly on the pinhole aperture $A_2$.

The spectrum of the scattered light was analyzed by a piezoelectrically-scanned Fabry-Perot spectrometer (Fig. 1). The circular entrance aperture $A_1$ had a diameter of ~4 mm, and limited the angular range over which light was collected to ~15 mrad, Lens $L_2$, which was located at its focal distance (280 mm) from the scattering volume, directed the light into the interferometer in a collimated beam. The Haidinger fringe pattern produced by the interferometer was imaged in the focal plane of lens $L_3$ ($f = 560$ mm) where its central portion was sampled by pinhole aperture $A_2$. $L_2$ and $L_3$ were high-quality camera lenses with focal lengths chosen to give a magnification of two at the pinhole.

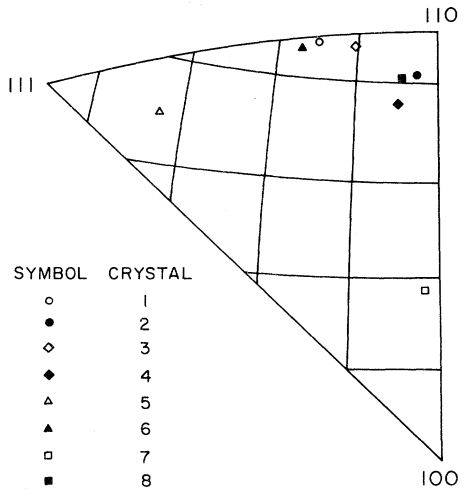


FIG. 4. Stereographic projection of $\frac{1}{48}$ of the reference sphere showing the direction of crystal growth (relative to the crystal axes) for each of the eight single crystals of neon.

The piezoelectrically scanned Fabry-Perot interferometer was the most critical component of the spectrometer. Its design and construction emphasizing long-term stability have already been described.[19] The mirrors used were flat to $\frac{1}{200}\lambda$ and dielectrically coated for a reflectivity of 98% at 4880 Å. Their spacing was $20.58 \pm 0.01$ mm which corresponds to a spectral free range of $7.284 \pm 0.004$ GHz. The over-all instrumental linewidth was ~100 MHz, and this was maintained during the course of each experiment. During an experiment the interferometer was repetitively scanned through ~0.45 $\mu$m or 1.7 interferometer orders, at a rate of 1 Hz, by applying a linearly increasing voltage to the piezoelectric translators. Light passing through pinhole $A_2$ was imaged by lens $L_4$, onto the photocathode of the photomultiplier tube (ITT FW-130). The signal was detected by a photon-counting system, and the spectrum accumulated, in 512 channels of a multichannel scaler (Northern Scientific 636). A digital stabilizer (Northern Scientific 453) compensated for any long-term frequency drift. After accumulation of data for 1 to 2 h, the memory contents were read out on a strip-chart recorder.

## III. EXPERIMENTAL RESULTS

### A. Brillouin spectra and measured frequency shifts

As discussed in the earlier work on xenon and argon, the Brillouin spectrum of a cubic crystal consists of a longitudinal doublet and two transverse doublets, and their intensities depend on the magnitudes of the photoelastic constants.

Three typical spectra of neon are shown in Fig. 5. These were recorded at three different orientations of crystal No. 6 (with rotation $\phi$ about the cell axis differing by ~20° and ~40°). All three spectra in Fig. 5 exhibit the longitudinal Brillouin doublet. The $T_1$ transverse doublet appears at $\phi = 222.9°$ and at $\phi = 242.6°$, but not at $\phi = 261.1°$. The $T_2$ transverse doublet does not appear in any of the spectra. It can be clearly seen that the frequency shifts of the components changed as the crystal was rotated. This is direct evidence of the elastic anisotropy of solid neon. More striking, however, is the variation in the relative intensities of the components. The intensity ratio between the $T_1$ and the longitudinal component $I(T_1)/I(L)$ is 0.17 at $\phi = 222.9°$ and 0.12 at $\phi = 242.6°$. At $\phi = 261.1°$ neither of the transverse components has sufficient intensity to be observed above the background. The strong unshifted component which appears in all of the spectra is due almost entirely to parasitic scattering.

A total of 29 spectra were obtained from the eight single crystals. The longitudinal Brillouin doublet appeared in all 29 spectra and the low-frequency transverse doublet ($T_1$) in 21. However, the high-frequency transverse doublet ($T_2$) was too weak to be detected in any of the spectra. The separations of these components from the central line were measured directly from the chart paper, and the frequency shifts were determined to an accuracy of 0.5% for $\nu(L)$ and 1% for $\nu(T_1)$.

The data obtained from all 29 spectra are presented in Table I, including crystal orientation, measured frequency shifts and uncertainties, and the intensity ratios $I(T_1)/I(L)$ determined from the peak intensities. Included in the Brillouin-shift uncertainties are both the measurement uncertainty discussed above, and also the "orientation uncertainty." The latter was obtained from computer analysis of the x-ray photographs in a manner similar to that described in Ref. 3. For each spectrum, the computer program determined the range of orientations permitted by the uncertainties in the positions of the Laue spots. Then, for each Brillouin component, the program used ap-

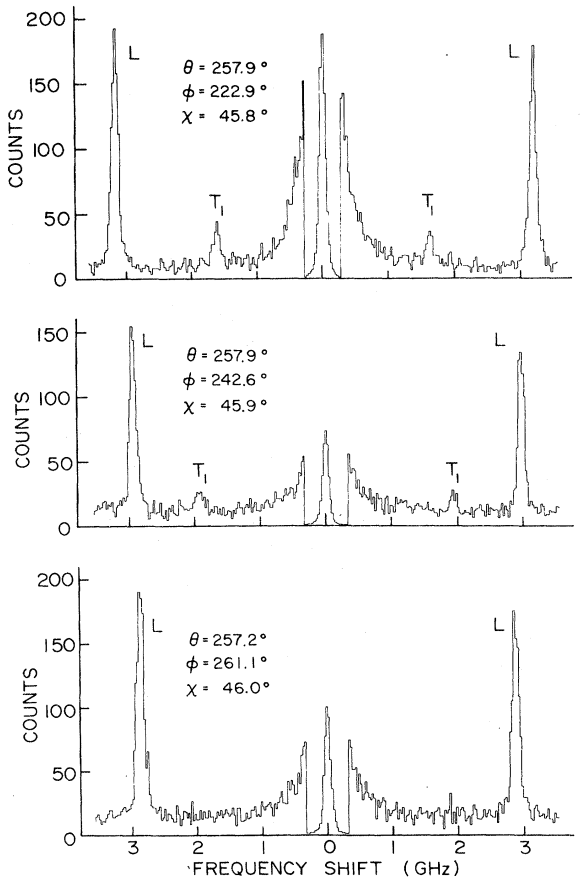


FIG. 5. Brillouin spectra of crystal No. 6 in three different orientations ($\theta$, $\phi$, $\chi$). (The central component in each spectrum has been attenuated by a factor of 64.)

TABLE I. Observed Brillouin shifts (in GHz) and intensity ratios as functions of orientation for the eight neon single crystals. The Euler angles $(\theta, \phi, \chi)$ are given in degrees.

| Crystal No. | $\theta$ | $\phi$ | $\chi$ | $\nu(L)$ | $\nu(T_1)$ | $I(T_1)/I(L)$ |
|---|---|---|---|---|---|---|
| 1 | 225.3 | 314.9 | 15.6 | 3.296 ± 0.046 | 1.480 ± 0.052 | 0.14 ± 0.04 |
| | 225.6 | 333.5 | 14.9 | 3.098 ± 0.053 | 1.758 ± 0.053 | 0.19 ± 0.04 |
| 2 | 310.8 | 44.9 | 2.9 | 3.279 ± 0.043 | ••• | ••• |
| | 310.5 | 46.0 | 2.6 | 3.294 ± 0.043 | 1.367 ± 0.055 | 0.10 ± 0.05 |
| | 310.2 | 61.8 | 2.6 | 3.368 ± 0.040 | ••• | ••• |
| | 311.2 | 62.5 | 2.8 | 3.372 ± 0.040 | ••• | ••• |
| 3 | 262.3 | 272.0 | 43.2 | 2.934 ± 0.032 | 2.036 ± 0.071 | 0.05 ± 0.03 |
| | 262.4 | 285.7 | 43.6 | 3.060 ± 0.037 | 1.778 ± 0.046 | 0.20 ± 0.04 |
| | 262.8 | 292.4 | 43.7 | 3.140 ± 0.041 | 1.660 ± 0.046 | 0.18 ± 0.05 |
| | 262.6 | 296.0 | 43.8 | 3.178 ± 0.032 | 1.602 ± 0.042 | 0.21 ± 0.04 |
| | 261.9 | 311.3 | 44.5 | 3.285 ± 0.033 | 1.363 ± 0.041 | 0.14 ± 0.04 |
| 4 | 266.1 | 54.3 | 52.3 | 3.208 ± 0.042 | ••• | ••• |
| | 266.1 | 69.1 | 51.8 | 3.066 ± 0.034 | ••• | ••• |
| 5 | 313.7 | 70.7 | 37.7 | 3.124 ± 0.031 | 1.696 ± 0.036 | 0.23 ± 0.05 |
| 6 | 257.9 | 215.1 | 45.3 | 3.273 ± 0.033 | 1.545 ± 0.030 | 0.18 ± 0.03 |
| | 257.9 | 222.9 | 45.8 | 3.185 ± 0.032 | 1.625 ± 0.031 | 0.17 ± 0.03 |
| | 257.6 | 236.8 | 45.7 | 3.030 ± 0.030 | 1.849 ± 0.048 | 0.17 ± 0.03 |
| | 257.9 | 242.6 | 45.9 | 2.980 ± 0.030 | 1.941 ± 0.037 | 0.12 ± 0.02 |
| | 257.4 | 251.4 | 45.9 | 2.894 ± 0.029 | ••• | ••• |
| | 257.9 | 251.5 | 46.0 | 2.899 ± 0.029 | ••• | ••• |
| | 257.2 | 261.1 | 46.0 | 2.893 ± 0.029 | ••• | ••• |
| | 257.5 | 268.8 | 46.0 | 2.940 ± 0.029 | 1.985 ± 0.040 | 0.09 ± 0.02 |
| | 257.4 | 280.3 | 46.4 | 3.054 ± 0.031 | 1.786 ± 0.036 | 0.15 ± 0.03 |
| | 257.2 | 286.3 | 46.7 | 3.132 ± 0.031 | 1.688 ± 0.035 | 0.18 ± 0.04 |
| 7 | 198.4 | −12.9 | 5.7 | 3.215 ± 0.032 | 1.599 ± 0.031 | 0.15 ± 0.02 |
| | 199.1 | 26.9 | 4.0 | 3.265 ± 0.033 | 1.591 ± 0.027 | 0.22 ± 0.04 |
| 8 | 266.8 | 249.2 | 48.9 | 3.001 ± 0.030 | 1.878 ± 0.034 | 0.14 ± 0.02 |
| | 266.3 | 283.4 | 49.5 | 3.018 ± 0.030 | 1.896 ± 0.036 | 0.14 ± 0.04 |
| | 266.7 | 300.4 | 49.8 | 3.174 ± 0.032 | 1.611 ± 0.035 | 0.18 ± 0.05 |

proximate values of the elastic constants to find the maximum variation in frequency shift which could occur over this range of orientations. The "orientation uncertainty" was set equal to this maximum variation. The measurement uncertainties and "orientation uncertainties" were combined to obtain the total uncertainties given in Table I. These were typically 1% for $\nu(L)$ and 2% for $\nu(T_1)$.

For six of the eight crystals, the number of spectra obtained was less than five. This would appear to be rather inefficient and requires some explanation. Crystal Nos. 1 and 2 were grown in preliminary experiments, and therefore, only a few spectra were recorded. In crystal Nos. 4, 5, 7, and 8, damage such as cracks and bubbles developed during the experiment, and the resulting parasitic scattering limited the number of spectra which could be obtained.

### B. Determination of the elastic constants

As explained in Refs. 1 and 3, the acoustic-mode frequencies $\omega_\mu(\vec{q})$ of a crystal are related to the eigenvalues $k_\mu$ of the dynamical matrix $A$ by $\omega_\mu(\vec{q}) = (k_\mu/\rho)^{1/2}$. The matrix elements of $A$ [Eq. (2), Ref. 3] depend on the wave vector $\vec{q}$ and on the adiabatic elastic constants, of which there are three ($C_{11}$, $C_{12}$, and $C_{44}$) for a cubic crystal. The Brillouin shifts $\omega_\mu(\vec{q})$ which occur for scattering vector $\vec{q}$ are identically equal to $\omega_\mu(\vec{q})/2\pi$; this relation leads directly to the Brillouin equation:

$$\nu_\mu(\vec{q}) = [2n v_\mu(\hat{q})/\lambda]\sin(\tfrac{1}{2}\alpha),$$

where $n$ is the refractive index of the crystal, $\lambda$ is the wavelength of the exciting radiation in vacuo, and $v_\mu(\hat{q}) = \omega_\mu(\vec{q})/|\vec{q}|$ is the acoustic-mode velocity.

The 29 values of $\nu(L)$ and 21 values of $\nu(T_1)$ presented in Table I will be denoted $\nu_i^{\rm obs}$, with the index $i$ running from 1 to 50. The corresponding uncertainties will be denoted $\sigma_i$. Once $\hat{q}$ had been evaluated for each spectrum, the calculated Brillouin shift $\nu_i^{\rm calc}$ corresponding to $\nu_i^{\rm obs}$ could be obtained as a function of assumed values of the elastic constants. The values of $n$ and $\rho$ which were used are given in Table II; and the scattering angles $\alpha$ (almost always 90°) were measured for each experiment to an accuracy of 15′. The elastic constants were determined by using the method

TABLE II. Physical constants of solid neon.

| | |
|---|---|
| Molecular weight | 20.183 g mole$^{-1}$ |
| Triple-point temperature [a] | 24.553 ± 0.001 K |
| Triple-point pressure [a] | 352.02 ± 0.10 Torr |
| Density [b] $\rho$ (24.3 K) | 1.4371 ± 0.0015 g cm$^{-3}$ |
| Lattice spacing [b] $a$ (24.3 K) | 4.537 Å |
| Volume expansivity [b] $\beta$ (24.3 K) | (57 ± 1) × 10$^{-4}$ K$^{-1}$ |
| Specific heat [c] $C_p$ (24.3 K) | 25 ± 1 J mole$^{-1}$ K$^{-1}$ |
| Refractive index [d] $n$ (24.3 K) | 1.107 ± 0.003 |

[a] Reference 20.
[b] Reference 21.
[c] Reference 22.
[d] See Appendix.

of least squares[23] to fit the calculated Brillouin shifts to the observed shifts. This involved minimizing the quantity $\chi^2(C_{11}, C_{12}, C_{44})$ with respect to variation of the $C_{ij}$'s.

$$\chi^2(a_1, a_2, a_3) = \sum_i \left( \frac{\nu_i^{\text{calc}}(a_1, a_2, a_3) - \nu_i^{\text{obs}}}{\sigma_i} \right)^2 ,$$

where $a_1 \equiv C_{11}$, $a_2 \equiv C_{12}$, and $a_3 \equiv C_{44}$. The sum extends over all shifts being used in the determination. The values $a_\gamma$ which minimize $\chi^2$ will be denoted $a_\gamma^*$, and the minimum value will be denoted $\chi^2_{\min}$. The minimization was performed by a computer program which used an iterative procedure based on Newton's method.[24] The covariances of the elastic constants were obtained from the error matrix $H$ where

$$(H^{-1})_{mn} = \left( \sum_i \frac{\partial \nu_i^{\text{calc}}}{\partial a_m} \frac{\partial \nu_i^{\text{calc}}}{\partial a_n} \frac{1}{\sigma_i^2} \right)_{a_\gamma^*} .$$

The uncertainties in the elastic constants are given by $\Delta C_{11} = (H_{11})^{1/2}$, $\Delta C_{12} = (H_{22})^{1/2}$, $\Delta C_{44} = (H_{33})^{1/2}$. The error matrix was calculated by the computer program as part of the minimization procedure.

All eight crystals were studied at the same temperature (24.3 K). The data from all of them were therefore combined to determine the "best values" of the elastic constants; these appear in the first row of Table III along with the uncertainties $\Delta C_{ij}$. Two checks were performed on the internal consistency of the results. In the first check, the constants were evaluated by using only the data of crystal No. 3 and then by using only the data of crystal No. 6. As shown in Table III, the values so obtained agree with each other and with the "best values." In the second check, the constants were evaluted by using only the longitudinal shifts and then by using only the transverse shifts. Once again there is good agreement with the "best values"; the uncertainties, however, are considerably larger. Table III also gives the number of Brillouin shifts, $N$, included in each determination of the constants.

TABLE III. Adiabatic elastic constants (in kbar) of solid neon at 24.3 K. $N$ is the number of Brillouin shifts included in each determination.

| | $N$ | $C_{11}$ | $C_{12}$ | $C_{44}$ |
|---|---|---|---|---|
| All crystals | 50 | 11.70 ± 0.09 | 7.31 ± 0.10 | 6.02 ± 0.09 |
| Crystal No. 3 only | 10 | 11.66 ± 0.23 | 7.31 ± 0.24 | 5.96 ± 0.26 |
| Crystal No. 6 only | 17 | 11.74 ± 0.12 | 7.29 ± 0.20 | 6.04 ± 0.14 |
| $\nu(L)$ only | 29 | 11.73 ± 0.11 | 7.30 ± 0.82 | 5.98 ± 0.41 |
| $\nu(T_1)$ only | 21 | 11.64 ± 0.58 | 7.31 ± 0.60 | 6.07 ± 0.14 |

The agreement obtained between the measured Brillouin shifts and those calculated from the "best values" is illustrated in Fig. 6 for crystals Nos. 3 and 6. For each crystal, the calculated values of $\nu(L)$, $\nu(T_1)$, and $\nu(T_2)$ have been plotted as functions of the Euler angle $\phi$. The measured Brillouin shifts and their uncertainties are indicated by the dots and error bars.

The uncertainties quoted in Table III for the elastic constants arise solely from the uncertainties in the Brillouin shifts (i.e., the combination of measurement and orientation uncertainties). An additional uncertainty in the constants results

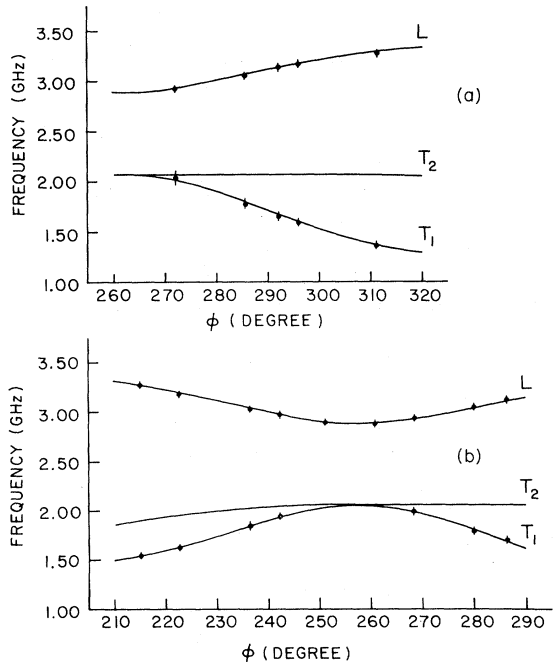


FIG. 6. Measured and calculated Brillouin shifts versus rotation angle $\phi$. The measured shifts and uncertainties are indicated by the dots and error bars, and the curves were calculated from the "best values" of the elastic constants (a) crystal No. 3, (b) crystal No. 6.

from uncertainties in the wavelength, spectral free range, density, refractive index, and scattering angle; errors in these quantities will scale the values obtained for all three elastic constants by the same factor. The wavelength was considered exact, the uncertainties in the spectral free range and $\alpha$ have been quoted previously, and the uncertainties in $\rho$, and $n$, are given in Table II. When all of these factors are combined, the increased uncertainty in each of the constants is ~1%. This amount was added to the uncertainties in the "best values" to obtain the total uncertainties in the elastic constants.

The final results for the adiabatic elastic constants of solid neon at 24.3 K are

$$C_{11} = 11.70 \pm 0.21 \text{ kbar},$$

$$C_{12} = 7.31 \pm 0.17 \text{ kbar},$$

$$C_{44} = 6.02 \pm 0.15 \text{ kbar}.$$

The adiabatic bulk modulus $B_s$, and the elastic anisotropy parameter $A$ are readily derived from the elastic constants. The values are

$$B_s = \tfrac{1}{3}(C_{11} + 2C_{12}) = 8.77 \pm 0.17 \text{ kbar},$$

$$A = 2C_{44}/(C_{11} - C_{12}) = 2.74 \pm 0.10.$$

The uncertainties in these quantities have been calculated by using the error matrix and the method of propagation of errors.[25]

### C. Elasto-optic coefficients

The relative intensities of the Brillouin components $I(T_1)/I(L)$ given in Table I together with the elastic constants and[26] Eq. (19) of Ref. 1 were used to obtain values of the ratios $p_{12}/p_{11}$ and $p_{44}/p_{11}$ of the elastic-optic coefficients. The procedure was completely analogous to that used to evaluate the elastic constants, above. The best agreement between the observed and calculated intensity ratios was obtained with

$$p_{12}/p_{11} = 1.35$$

and

$$p_{44}/p_{11} = -0.10.$$

However, reasonable agreement was also obtained with $p_{12}/p_{11} = 0.85$ and $p_{44}/p_{11} = 0.11$, and with a large number of other combinations between these two sets. It was concluded therefore that the available data were too inaccurate and limited to allow a reliable determination of these ratios. For all 29 spectra the value of $I(T_2)/I(L)$ predicted by this analysis was less than 0.04, which explains why the $T_2$ component was not observed.

## IV. DISCUSSION

### A. Comparison of available experimental values

Prior to this experiment, the only known values of the elastic constants of solid neon were those determined at higher densities from inelastic neutron-scattering experiments. The first such experiment was reported by Leake *et al.*[27] Subsequent technical advances permitted Skalyo *et al.*[28] to perform similar experiments with a threefold improvement in accuracy. Their results are listed in Table IV along with the present values. The large increase in the elastic constants with increasing density indicates the importance of anharmonicity in solid neon. It should be noted, however, that values of elastic constants in such anharmonic solids obtained by Brillouin and neutron scattering may not be directly comparable because of the distinction between first and zero sound, as discussed in the work on krypton.[4,29]

The only experimental datum which may be directly compared with the present results is the value of the adiabatic bulk modulus $B_s$ obtained from ultrasonic experiments with polycrystalline specimens. Bezuglyi *et al.*[30] have measured the propagation velocities of longitudinal and transverse ultrasonic waves ($v_L$ and $v_T$, respectively) in neon polycrystals over the temperature range 2–20 K. Balzer *et al.*[31] have made similar measurements from 18.5 to 24.5 K and have combined their results with those of Bezuglyi *et al.*[30] to obtain smoothed values of $v_L$ and $v_T$ from 0 K up to the triple point. From the sound-velocity data, they have calculated $B_s$ using the following formula, which is valid for an isotropic solid: $B_s = \rho(v_L^2 - \frac{4}{3}v_T^2)$. Their value at 24.3 K is $B_s = 7.50 \pm 0.38$ kbar which is 14% lower than that obtained in the present experiment. To investigate the reason for this discrepancy, we have used the present values of the elastic constants and the expressions given by Barron and Klein [Eq. (3.20) of Ref. 32] to estimate $v_L$ and $v_T$ for polycrystalline neon. These estimates show that the ultrasonic value for $v_T$ is much too high (603 compared with 530 m/sec) to be

TABLE IV. Experimental values of the elastic constants and elastic anisotropy $A$ of solid neon.

| | Temp. (K) | Lattice spacing (Å) | $C_{11}$ (kbar) | $C_{12}$ (kbar) | $C_{44}$ (kbar) | $A$ |
|---|---|---|---|---|---|---|
| Neutron scattering[a] | 5 | 4.454 | 16.61 | 8.55 | 9.52 | 2.36 |
| | 22 | 4.454 | 16.77 | | 8.85 | |
| Present results | 24.3 | 4.537 | 11.70 | 7.31 | 6.02 | 2.74 |

[a] Reference 28.

consistent with a truly isotropic specimen in the ultrasonic experiments.

Figure 7 shows $B_s$ as determined in this experiment at 24.3 K, and as obtained from the ultrasonic work over the entire temperature range from 0 to 24.5 K. Several other experimental values for $B_s$ have been included on the graph even though they are not directly comparable with the present results because of the differences in temperature. Among these are the results of Anderson *et al.*,[33] who obtained values of the isothermal bulk modulus $B_T$ at 4.2, 13.5, and 19.9 K by extrapolation of piston-displacement equation-of-state data. The corresponding values for $B_s$ have been derived by applying the adiabatic-isothermal correction from Ref. 31. Also included on the graph is the value of $B_T$ at 4.25 K obtained by Batchelder *et al.*[21] using an x-ray-diffraction technique. At this temperature, the adiabatic-isothermal correction is negligible. The neutron-scattering result of Skalyo *et al.*[28] at 5 K has been corrected to the zero-pressure lattice spacing as described in their paper. The graph also shows the results of four theoretical calculations discussed below.

The thermal Grüneisen parameter $\gamma$ is given by $\gamma = \beta V B_s / C_p$, where $\beta$ is the volume expansivity, $V$ is the molar volume, and $C_p$ is the specific heat at constant pressure. Substitution of $\beta$, $V$, and $C_p$ as given in Table II, and of $B_s$ as determined in the present experiment, yields $\gamma = 2.80 \pm 0.15$. This is in good agreement with the value $\gamma = 2.76$ at 24.3 K determined by Anderson *et al.*[33] from equation-of-state data.

### B. Review of theoretical calculations of elastic constants, and comparison with experimental values

A number of different lattice-dynamic models have been used to calculate the elastic constants of neon, and the results are summarized in Table V and Fig. 8.

Barron and Klein[32] calculated the elastic constants of solid neon at 0 K in the quasiharmonic (QH) approximation using both a nearest-neighbor (NN) and an all-neighbor (AN) Mie-Lennard-Jones potential (MLJ). The usefulness of the QH approximation for calculating the high-temperature properties of the rare-gas solids was investigated by Holt *et al.*[34] They used an MLJ (6-12) AN potential to calculate the elastic constants of neon over the entire temperature range from 0 K to the triple point. The agreement with the present experimental results is impressive (Table V); the theoretical values for $C_{11}$ and $C_{44}$ are ~5% greater and ~4% smaller, respectively, than the experimental values, while the calculated and experimental values for $C_{12}$ are equal.

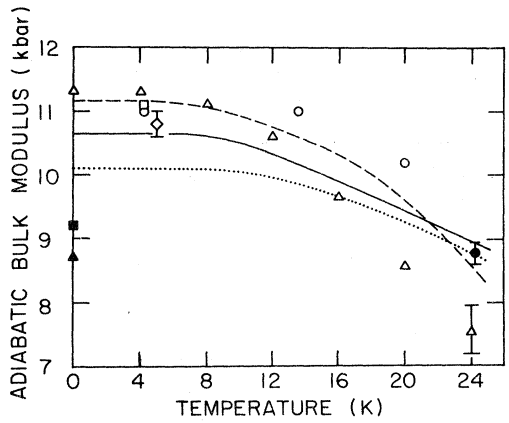


FIG. 7. Adiabatic bulk modulus of solid neon as a function of temperature. The experimental values are from ● present work; △ ultrasonics (Ref. 31); □ x-ray diffraction (Ref. 21); ◇ neutron diffraction (Ref. 28); ○ piston displacement (Ref. 33). The theoretical curves are (——) the QH calculations of Holt *et al.* (Ref. 34) based on a MLJ (6–12) AN potential; (• • • •) the SC calculations of Klein *et al.* (Ref. 37) based on a MLJ (6–12) NN potential; (----) the SC calculations of Klein (Ref. 42) based on a MSV AN potential and three-body forces. The values at 0 K are the QH results of Barron and Klein (Ref. 32) for a MLJ (6–12) NN (▲) and AN (■) potential.

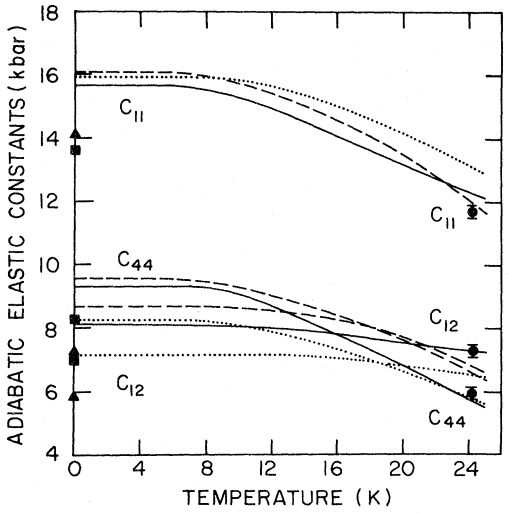


FIG. 8. Adiabatic elastic constants of solid neon as a function of temperature. The present experimental values are plotted as solid dots. The theoretical curves are (——) the QH calculations of Holt *et al.* (Ref. 34) based on a MLJ (6–12) AN potential; (• • • •) the SC calculations of Klein *et al.* (Ref. 37) based on a MLJ (6–12) NN potential; (----) the SC calculations of Klein (Ref. 42) based on a MSV AN potential and three-body forces. The values at 0 K are the QH results of Barron and Klein (Ref. 32) for a MLJ (6–12) NN(▲) and AN(■) potential.

TABLE V. Theoretical values of the adiabatic elastic constants, the adiabatic bulk modulus, and the elastic anisotropy parameter $A$ for solid neon.

| | Theory | Potential | Temp. (K) | $C_{11}$ (kbar) | $C_{12}$ (kbar) | $C_{44}$ (kbar) | $B_s$ (kbar) | $A$ |
|---|---|---|---|---|---|---|---|---|
| Barron and Klein [a] | QH | MLJ (6-12) NN | 0 | 14.1 | 5.9 | 7.3 | 8.7 | 1.8 |
| | QH | MLJ (6-12) AN | 0 | 13.6 | 7.0 | 8.3 | 9.2 | 2.5 |
| Holt, Hoover, Gray, and Shortle [b] | QH | MLJ (6-12) AN | 24.3 | 12.3 | 7.3 | 5.8 | 9.0 | 2.3 |
| Klein, Horton and Goldman [c] | SC | MLJ (6-12) NN | 24.3 | 13.1 | 6.5 | 5.8 | 8.7 | 1.8 |
| Klein [d] | SC | MSV AN and three-body forces | 24.3 | 11.98 | 6.83 | 6.48 | 8.55 | 2.52 |
| Present results | | | 24.3 | 11.70 ± 0.21 | 7.31 ± 0.17 | 6.02 ± 0.15 | 8.77 ± 0.17 | 2.74 ± 0.10 |

[a] Reference 32.
[b] Reference 34.
[c] Reference 37.
[d] Reference 42.

The theory of self-consistent (SC) phonons[35] provides a more adequate treatment of large-amplitude lattice vibrations. With this approach, much better agreement has been obtained between theoretical and experimental values of thermodynamic properties of the rare-gas solids, particularly at high temperatures.[36] Klein *et al.*[37] have calculated the isothermal elastic constants of solid neon as functions of temperature using the first-order self-consistent theory and a MLJ (6-12) NN potential. The corresponding adiabatic elastic constants and bulk modulus are shown by the dotted curves in Figs. 7 and 8, and the values obtained at 24.3 K appear in Table V (The adiabatic-isothermal corrections were obtained from Ref. 31.) The agreement with the present experimental results is relatively poor. The theoretical value of $C_{11}$ is greater than the experimental value by ~12%, while the theoretical values of $C_{12}$ and $C_{44}$ are smaller than the experimental values by ~11 and ~4%, respectively. Excellent agreement is found for the bulk modulus, however, since the discrepancies in $C_{11}$ and $C_{12}$ cancel each other.

As discussed above, the MLJ (6-12) AN pair potential gives quite accurate predictions for the adiabatic elastic constants of solid neon at 24.3 K. This same potential also gives good predictions for the temperature shifts of the phonon frequencies[38] and for the $pV$ isotherms at 0 K.[39] The ability of the MLJ (6-12) AN potential to correlate such a large amount of solid-state data is surprising for several reasons. First of all, it has been known for some time that the (6-12) potential does not give a satisfactory description of dilute gas properties.[40] Furthermore, the coefficient of $R^{-6}$ in this potential is 50% larger than predicted theoretically.[41] Finally, it is known that many-body forces (i.e., nonpairwise additive forces) are present in solid neon, although their importance is relatively smaller here than in the heavier rare-gas solids.[13-15]

Recently, experiments have been carried out which provide precise information on the neon pair potential. Siska *et al.*[9] have reported high-resolution measurements of differential scattering cross sections for Ne + Ne in molecular-beam experiments. Farrar *et al.*[10] have extended these measurements to obtain more accurate information on the attractive part of the potential. Tanaka and Yoshino[8] have investigated the absorption spectrum of $Ne_2$ in the 585–760-Å region and have found two vibrational levels in the ground state, with a spacing of 13.7 $cm^{-1}$. All of these experiments have confirmed the fact that the MLJ (6-12) potential gives a poor representation of the pair interaction between neon atoms.

To fit their molecular-beam data, Siska *et al.*[9] proposed a potential whose bowl and repulsive wall were given by a Morse function and whose long-range behavior was taken from theoretical calculations of the Van der Waals attraction.[41] The two parts were joined by cubic spline interpolation, and the resulting potential was called a Morse–spline–Van der Waals (MSV) potential. Goldman and Klein[12] have derived two neon pair potentials of the MSV form from solid-state data, and Klein[42] has used one of these together with the Axilrod-Teller-Muto (ATM) triple-dipole interaction[43] in a SC calculation of the adiabatic elastic constants of solid neon. The results for the entire temperature range from 0 K up to the triple point are shown by the dashed curves in Figs. 7 and 8 and the values obtained at 24.3 K are given in Table V. The calculated values of $C_{11}$ and $C_{44}$ are larger than the present experimental values by ~2 and ~7%, respectively, while the calculated

value of $C_{12}$ is smaller than the experimental value by ~7%. Although these discrepancies are considerably larger than the present experimental uncertainties, they are not large enough to rule out MSV as a viable pair potential for neon since one must also consider the inaccuracies inherent in the SC approximation. The work of Klein and Hoover[44] has shown that adiabatic elastic constants obtained from SC calculations may be in error by as much as 5% near the triple point. Consequently, the uncertainties in the SC elastic constants when combined with the present experimental uncertainties could account for the observed discrepancies. A similar situation exists with respect to the many-body forces. The contribution of the ATM triple-dipole force to $C_{11}$ and $C_{12}$ is ~5%, which is larger than the experimental errors. However, the uncertainty in the pair potential together with the inaccuracy in the SC calculations makes it impossible to use the elastic constant-data to assess the validity of the ATM interaction for solid neon. What is clearly needed is a technique for calculating the elastic constants of neon near the triple point to an accuracy of ~2%.

Recently, Monte Carlo (MC) methods have been used to calculate the properties of solid argon,[44-47] krypton,[46] and xenon.[44,46] These calculations take all interactions into account (within the assumption of a given force law) and in principle provide an exact solution to the dynamical problem. The MC calculations are classical, however, and quantum corrections must be added. For argon, krypton, and xenon, these corrections are small at high temperatures, and the MC approach is a useful one since elastic constants may be calculated to an accuracy of ~2%. For neon, however, the quantum corrections are large even at the triple point, approximately 16, 6, and 25% for $C_{11}$, $C_{12}$, and $C_{44}$, respectively.[34] Consequently, the MC approach, at least in its present form, is probably not useful for solid neon.

## V. CONCLUSIONS

The elastic constants of neon determined here are the only available values for the solid under its own vapor pressure. These results lead to a large anisotropy of the elasticity, ~2.7, just as found for xenon and argon crystals. Agreement with theoretical calculations seems best for values using the quasiharmonic approximation and a Mie-Lennard-Jones (6-12) all-neighbor potential. Nevertheless, the agreement is not as satisfactory as found for solid argon, and indicates the desirability of further theoretical work.

On the experimental side, improvements in techniques now make possible the investigation of light scattering from very weak sources, such as neon at low temperatures. Higher accuracy in the evaluation of the elastic constants of crystals requires more refined x-ray-diffraction techniques than used here for determining the crystal orientations. Finally, just as found with xenon and argon crystals, it was not possible to cool the neon crystals appreciably below the freezing point without shattering them. Thus the investigation of the Brillouin spectrum of a rare-gas crystal over a large range of temperatures remains an exciting challenge.

## ACKNOWLEDGMENTS

The authors wish to acknowledge helpful discussions with M. L. Klein, W. S. Gornall, S. Gewurtz, G. I. A. Stegeman, and G. Enright during the course of this investigation. They would also like to thank A. Jares and P. Allen for their technical assistance, and R. Munnings for advice on the temperature controller.

## APPENDIX: CALCULATION OF REFRACTIVE INDEX

A measured value for the refractive index of solid neon is not available. However, it was possible to calculate a value by using the Lorentz-Lorenz relation and measurements of the dielectric constant of liquid neon.[48] This calculation can be explained very simply by introducing the Lorentz-Lorenz function $f_{LL}$ and defining

$$f_{LL}(\text{liquid, static}) = \left(\frac{\epsilon(\text{liq})-1}{\epsilon(\text{liq})+2}\right)\frac{1}{\rho(\text{liq})}, \tag{1}$$

$$f'_{LL}(\text{solid, optical}) = \left(\frac{n^2(\text{sol})-1}{n^2(\text{sol})+2}\right)\frac{1}{\rho(\text{sol})}, \tag{2}$$

where $\epsilon$(liq) is the static dielectric constant of the liquid and $n$(sol) is the optical refractive index of the solid. The assumption is then made that $f_{LL}=f'_{LL}$ giving the relationship between $n$(sol) and $\epsilon$(liq),

$$\left(\frac{n^2(\text{sol})-1}{n^2(\text{sol})+2}\right) = \left(\frac{\epsilon(\text{liq})-1}{\epsilon(\text{liq})+2}\right)\frac{\rho(\text{sol})}{\rho(\text{liq})}. \tag{3}$$

At 25 K, $\epsilon(\text{liq}) = 1.194 \pm 0.001$,[48] and $\rho(\text{liq}) = 1.243 \pm 0.002$ g/cm$^3$.[49] At 24.3 ±0.2 K, $\rho(\text{sol}) = 1.4371 \pm 0.0015$ gm/cm$^3$ (Table II). Substitution of these values into Eq. (3) yields $n(\text{sol}) = 1.107$.

This calculation depends on the validity of Eq. (3), which is based on two separate assumptions. The first assumption is that $f_{LL}$ has the same value for the solid as it does for the liquid. This is a special case of the Lorentz-Lorenz relation, which states that for a homogeneous nonpolar medium, $f_{LL}$ is independent of density. Sinnock and

Smith[50] have made extensive refractive-index measurements for the condensed phases of Ar, Kr, and Xe. They found that $f_{LL}$ actually decreases by ~1% when these substances freeze. The second assumption is that there is no dispersion between the static and optical values for $f_{LL}$. A comparison of the dielectric-constant measurements of Amey and Cole[51] with the refractive-index measurements of Sinnock and Smith (at ~5000 Å) reveals that for liquid Ar, Kr, and Xe, $f_{LL}(\text{static}) < f_{LL}(\text{optical})$ by 1.8, 3.7, and 8.5%, respectively. It seems reasonable to assume that for neon this difference is ~1%. This assumption is supported by the results of Cuthbertson and Cuthbertson[52] on the refractive index of gaseous neon, which also imply a dispersion of ~1% in $f_{LL}$. Furthermore, it should be noted that the change in $f_{LL}$ which occurs on freezing is in the opposite direction to that which results from dispersion. It may be safely assumed, therefore, that $f_{LL} = f'_{LL}$ is valid to an accuracy of at least 2%. When this figure is combined with the uncertainties in $\epsilon$(liq), $\rho$(liq), and $\rho$(sol), the uncertainty in $n$(sol) is found to be ~0.25%. The final result is therefore $n(\text{sol}) = 1.107 \pm .003$ at 24.3 K.

---

*Research supported in part by the National Research Council of Canada and the University of Toronto. The work reported here is based on the thesis by R. A. McLaren submitted for the Ph.D. degree to the University of Toronto in 1973. Brief preliminary reports of this work have been presented at a meeting of the Canadian Association of Physicists [Bull. Can. Assoc. Phys. 27, 30 (1971)] and in Ref. 2.

†Holder of a National Research Council of Canada Scholarship 1970-72, and of the Kodak of Canada Fellowship 1972-73. Present address: Department of Physics, University of California, Berkeley, Calif. 94720.

‡Post-Doctorate Fellow 1970-72. Present address: Department of Physics, Memorial University, St. John's, Newfoundland.

§Holder of a National Research Council of Canada "1967 Science" Scholarship, 1970-73.

[1]W. S. Gornall and B. P. Stoicheff, Phys. Rev. B 4, 4518 (1971).

[2]S. Gewurtz, H. Kiefte, D. Landheer, R. A. McLaren, and B. P. Stoicheff, Phys. Rev. Lett. 29, 1768 (1972).

[3]S. Gewurtz and B. P. Stoicheff, Phys. Rev. B 10, 3487 (1974).

[4]Howard E. Jackson, D. Landheer, and B. P. Stoicheff, Phys. Rev. Lett. 31, 296 (1973).

[5]L. H. Nosanow, Phys. Rev. 146, 120 (1966).

[6]N. R. Werthamer, Am. J. Phys. 37, 763 (1969); V. V. Goldman, G. K. Horton, and M. L. Klein, J. Low Temp. Phys. 1, 391 (1969).

[7]W. J. Mullin, Phys. Rev. 134, A1249 (1964); T. R. Koehler, Phys. Rev. Lett. 17, 89 (1966); N. D. Gillis, N. R. Werthamer, and T. R. Koehler, Phys. Rev. 165, 951 (1968); T. R. Koehler, Phys. Rev. Lett. 22, 77 (1969); J. P. Hansen, Phys. Rev. 172, 919 (1968); G. Meissner and J. P. Hansen, Phys. Lett. A 30, 61 (1969); V. V. Goldman, G. K. Horton, and M. L. Klein, Phys. Rev. Lett. 24, 1424 (1970).

[8]Y. Tanaka and K. Yoshino, J. Chem. Phys. 57, 2964 (1972).

[9]P. E. Siska, J. M. Parson, T. P. Shafer, and Y. T. Lee, J. Chem. Phys. 55, 5762 (1971).

[10]J. M. Farrar, Y. T. Lee, V. V. Goldman, and M. L. Klein, Chem. Phys. Lett. 19, 359 (1973).

[11]M. L. Klein, Chem. Phys. Lett. 18, 203 (1973).

[12]V. V. Goldman and M. L. Klein, J. Low Temp. Phys. 12, 101 (1973).

[13]B. M. Axilrod and E. Teller, J. Chem. Phys. 11, 299 (1943); B. M. Axilrod, *ibid.* 17, 1349 (1949); 19, 719 (1951); 19, 724 (1951); Y. Muto, J. Phys. Soc. Jap. 17, 629 (1943).

[14]I. J. Zucker, Nuovo Cimento B 54, 177 (1968); G. G. Chell and I. J. Zucker, J. Phys. C 1, 35 (1968); I. J. Zucker and G. G. Chell, *ibid.* 1, 1505 (1968); J. A. Barker, M. L. Klein, M. V. Bobetic, I. J. Zucker, M. B. Doran, and G. G. Chell, *ibid.* 4, L355 (1971); M. B. Doran and I. J. Zucker, *ibid.* 4, 307 (1971); I. J. Zucker and M. B. Doran, *ibid.* 5, 2302 (1972).

[15]M. L. Klein and R. J. Munn, J. Chem. Phys. 47, 1035 (1967).

[16]M. V. Bobetic and J. A. Barker, Phys. Rev. B 2, 4169 (1970); J. A. Barker, M. L. Klein, and M. V. Bobetic, *ibid.* 2, 4176 (1970).

[17]D. N. Batchelder, D. L. Losee, and R. O. Simmons, in *Crystal Growth*, edited by H. S. Peiser (Pergamon, New York, 1967), p. 843; Phys. Rev. 162, 767 (1967).

[18]R. A. McLaren and G. I. A. Stegeman, Appl. Opt. 12, 1396 (1973).

[19]A. Jares, M. Kostilek, R. A. McLaren and B. P. Stoicheff (unpublished).

[20]G. T. Furukawa, W. G. Saba, D. M. Sweger, and H. H. Plumb, Metrologia 6, 35 (1970).

[21]D. N. Batchelder, D. L. Losee, and R. O. Simmons, Phys. Rev. 162, 767 (1967).

[22]R. Q. Fugate and C. A. Swenson, J. Low Temp. Phys. 10, 317 (1973).

[23]Siegmund Brandt, *Statistical and Computational Methods in Data Analysis* (Elsevier, New York, 1970), Chap. 9.

[24]J. Kowalik and M. R. Osborne, *Methods for Unconstrained Optimization Problems* (Elsevier, New York, 1968), p. 65.

[25]Reference 23, p. 31.

[26]Equation (19) of Ref. 1 perpetuates an earlier error in which $p_{44}$ is taken to be twice its value. In the present work, this error has been corrected. See N. R. Werthamer, Phys. Rev. B 6, 4075 (1972).

[27]J. A. Leake, W. B. Daniels, J. Skalyo, Jr., B. C. Frazer, and G. Shirane, Phys. Rev. 181, 1251 (1969).

[28]J. Skalyo, Jr., V. J. Minkiewicz, and G. Shirane, Phys. Rev. B 6, 4766 (1972).

[29]D. Landheer, Howard E. Jackson, R. A. McLaren, and B. P. Stoicheff (unpublished).

[30]P. A. Bezuglyi, R. O. Plakhotin, and L. M. Tarasenko, Fiz. Tverd. Tela 12, 1199 (1970) [Sov. Phys.—Solid State 12, 934 (1970)].

[31]R. Balzer, D. S. Kupperman, and R. O. Simmons, Phys. Rev. B 4, 3636 (1971).

[32]T. J. K. Barron and M. L. Klein, Proc. Phys. Soc. Lond. 85, 533 (1965).

[33]M. S. Anderson, R. Q. Fugate, and C. A. Swenson, J. Low Temp. Phys. 10, 345 (1973).
[34]A. C. Holt, W. G. Hoover, S. G. Gray, and D. R. Shortle, Physica 49, 61 (1970).
[35]See, for example, P. F. Choquard, *The Anharmonic Crystal* (Benjamin, New York, 1967); N. R. Werthamer, Phys. Rev. B 1, 572 (1970); H. R. Glyde and M. L. Klein, Crit. Rev. Solid State Sci. 2, 181 (1971).
[36]M. L. Klein, V. V. Goldman, and G. K. Horton, J. Phys. Chem. Solids 31, 2441 (1970).
[37]M. L. Klein, G. K. Horton, and V. V. Goldman, Phys. Rev. B 2, 4995 (1970).
[38]T. R. Koehler, Phys. Rev. Lett. 22, 777 (1969).
[39]J. P. Hansen, Phys. Rev. 172, 919 (1968).
[40]T. Kihara, Rev. Mod. Phys. 25, 831 (1953); R. J. Munn and F. J. Smith, J. Chem. Phys. 43, 3998 (1965).
[41]G. Starkschall and R. G. Gordon, J. Chem. Phys. 54, 663 (1971); 56, 2801 (1972).
[42]M. L. Klein (unpublished).
[43]B. M. Axilrod and E. Teller, J. Chem. Phys. 11, 299 (1943); B. M. Axilrod, *ibid.* 19, 719 (1951); W. Götze and H. Schmidt, Z. Phys. 192, 409 (1966).
[44]M. L. Klein and W. G. Hoover, Phys. Rev. B 4, 537 (1971).
[45]D. R. Squire, A. C. Holt, and W. G. Hoover, Physica 42, 388 (1969); 42, 437 (1969); R. A. Fisher and R. O. Watts, Mol. Phys. 23, 1051 (1972).
[46]M. L. Klein and R. D. Murphy, Phys. Rev. B 6, 2433 (1972).
[47]T. G. Gibbons, M. L. Klein, and R. D. Murphy, Chem. Phys. Lett. 18, 325 (1973); J. A. Barker and M. L. Klein, Phys. Rev. B 7, 4707 (1973).
[48]L. Bewilogua, A. Handstein, and H. Hoeger, Cryogenics 6, 21 (1966).
[49]C. Gladun, Cryogenics 6, 27 (1966).
[50]A. C. Sinnock and B. L. Smith, Phys. Rev. 181, 1297 (1969).
[51]R. L. Amey and R. H. Cole, J. Chem. Phys. 40, 146 (1964).
[52]C. Cuthbertson and M. Cuthbertson, Proc. R. Soc. Lond. A 135, 40 (1932).